Defect and Diffusion Forum Vols. 273-276 (2008) pp 75-80
online at http://www.scientific.net
© (2008) Trans Tech Publications, Switzerland
Online available since 2008/Feb/11

The Enhanced Kinetics of Precipitation Effects in Ultra Fine Grained Mg Alloys Prepared by High Pressure Torsion

Jakub Cizek[1,a], Ivan Prochazka[1,b], B. Smola[1,c], I. Stulikova[1,d], V. Ocenasek[2,e], R.K. Islamgaliev[3,f], O. Kulyasova[3,g],

[1]Faculty of Mathematics and Physics, Charles University, V Holesovickach 2, CZ-180 00 Praha 8, Czech Republic

[2]Research Institute of Metals, Panenske Brezany 50, CZ-25070 Odolena Voda, Czech Republic

[3]Institute of Physics of Advanced Materials, Ufa State Aviation Technical University, Ufa 450 000, Russia

[a]jakub.cizek@mff.cuni.cz, [b]ivan.prochazka@mff.cuni.cz, [c]smola@met.mff.cuni.cz, [d]stulik@karlov.mff.cuni.cz, [e]ocenasek.vuk@volny.cz, [f]saturn@mail.rb.ru, [g]elokbox@mail.ru

Keywords: Mg hardenable alloys, positron annihilation spectroscopy, ultra fine grained materials, precipitation effects, high pressure torsion, severe plastic deformation

Abstract. Precipitation effects in ultra fine grained (UFG) lightweight Mg-based alloys were studied in the present work by means of positron lifetime spectroscopy, transmission electron microscopy, and microhardness. The UFG samples with grain size around 100 nm were fabricated by high pressure torsion (HPT). The UFG structure contains a significant volume fraction of grain boundaries and exhibits a high number of lattice defects (mainly dislocations) introduced by severe plastic deformation during the HPT processing. A high dislocation density and volume fraction of grain boundaries enhance the long range diffusion of solute elements. Moreover, dislocations and grain boundaries act as nucleation centers for precipitates. As a consequence, the precipitation effects are facilitated in the UFG alloys compared to the conventional coarse-grained samples. This phenomenon was examined in this work by comparison of the precipitation sequence in Mg alloys with UFG structure and solution treated coarse-grained alloys.

Introduction

Lightweight Mg-based alloys allow for a significant weight reduction which is important especially in automotive or aeronautical applications. However, use of conventional Mg-based alloys is limited due to a degradation of their mechanical properties at elevated temperatures. Improved mechanical properties even at temperatures around 300°C were achieved using heavy rare earth metal alloying elements [1]. The Mg-Gd and Mg-Tb-Nd systems are novel Mg-based light hardenable alloys with a high creep resistance at elevated temperatures. A remarkable precipitation hardening is achieved during decomposition of the supersaturated solid solution (sss) in these alloys [2,3]. In Mg-Gd alloys sss decomposes with increasing temperature into the following successive phases [2]: β'' (D019) → β' (c-bco) → β (fcc, stable). The decomposition sequence of Mg-Tb-Nd alloy undergoes the sequence typical for Mg-Tb system [3]: β'' (D019) → β_1 (fcc) → β (cubic, stable). Formation of fine precipitates of metastable phases can cause a significant hardening. In Mg-Gd alloys the peak hardening is achieved by precipitation of finely dispersed semicoherent β' phase [2]. The strongest hardening effect in Mg-Tb-Nd alloys is due to fine plates of coherent β'' precipitates [4].

Despite the favorable strength and thermal stability, a disadvantage of the new Mg alloys consists in ductility insufficient for most of the industrial applications. Grain refinement is a well-known method to improve ductility of metallic materials. An extreme grain size reduction can be obtained by severe plastic deformation (SPD), see [5] for a review. The methods based on SPD produce bulk materials with ultra fine grained (UFG) structure. The largest grain refinement was achieved by high pressure torsion (HPT) [5]. Small grain size (in the nanocrystalline range) leads to

All rights reserved. No part of contents of this paper may be reproduced or transmitted in any form or by any means without the written permission of the publisher: Trans Tech Publications Ltd, Switzerland, www.ttp.net. (ID: 89.176.102.73-08/03/08,22:07:21)

a significant volume fraction of grain boundaries which represent obstacles for movement of dislocations. It causes a significant hardening of UFG metals in addition to the age hardening effect caused by fine precipitates. As a consequence, the UFG metals exhibit a favorable combination of a very high strength and a reasonable ductility. The precipitation effects are influenced by concentration of nucleation sites and by the diffusivity of solutes. An increase in dislocation density leads to an increase of both parameters and can, therefore, facilitate the precipitation processes. For example, the effect of preliminary deformation on precipitation process was observed in Mg-15wt.%Gd alloy [6]. In the present work we compared precipitation processes in UFG and solution treated (coarse-grained) samples of Mg-9wt.%Gd (Mg9Gd) and Mg-3wt.%Tb-2wt.%Nd (Mg3Tb2Nd) alloy.

A high number of defects is created in the UFG specimens in the course of HPT processing. These defects play an important role in the precipitation effects in UFG materials. In this work we employed positron lifetime (PL) spectroscopy for defect studies on the atomic scale. The PL spectroscopy is a well developed non-destructive technique with a high sensitivity to open volume defects (e.g. vacancies, dislocations etc.) [7]. It enables to determine the nature of defects and defect concentration in studied material. In the present work, PL spectroscopy was combined with transmission electron microscopy (TEM) and microhardness measurements.

Experimental Details

The Mg9Gd and Mg3Tb2Nd alloys were prepared by squeeze casting. The chemical compositions of the alloys and the original Mg material used for casting are given in Table 1. The as-cast materials were subjected to 6 h solution annealing at 500^{o}C and 525^{o}C for Mg9Gd and Mg3Tb2Nd, respectively. This treatment is sufficient to dissolve the alloying elements completely in the Mg matrix [8]. To fabricate the UFG structure, the solution treated Mg9Gd and Mg3Tb2Nd alloys were deformed by HPT at room temperature using 5 rotations under a high pressure of 6 GPa. After characterization of the as deformed microstructure, the specimens were subjected to step-by-step isochronal annealing (20^{o}C / 20 min). Each annealing step was finished by quenching into water at room temperature and subsequent investigations performed at room temperature.

A fast-fast PL spectrometer similar to that described in [9] with time resolution of 160 ps was used in this work. At least 10^7 annihilation events were accumulated in each PL spectrum using ≈1 MBq ^{22}NaCl positron source on 2 μm thick mylar foil. The TEM observations were carried out on a JEOL 2000 FX electron microscope operating at 200 kV. The Vickers microhardness, HV, was measured at a load of 100 g applied for 10 s using STRUERS Duramin 300 hardness tester.

Material	Gd	Tb	Nd	Mn	Fe	Zn	Al	Si	Cu	Ni	Mg
Mg	-	-	-	0.014	0.020	0.0001	0.0077	0.0090	0.0026	0.0004	balance
Mg9Gd	9.33	-	-	0.014	0.020	0.0001	0.0077	0.0090	0.0026	0.0004	balance
Mg4Tb2Nd	-	3.15	1.75	0.014	0.020	0.0001	0.0077	0.0090	0.0026	0.0004	balance

Table 1. Chemical composition (in weight %) of the studied materials.

Results and Discussion

The PL results for the solution treated specimens and HPT deformed specimens are shown in Table 2. The solution treated Mg3Tb2Nd alloy exhibits a single component spectrum with the lifetime consistent with the bulk positron lifetime in a well annealed pure Mg. Thus, defect density in this alloy is extremely low and it can be considered as a defect-free material, which contains only defects allowed by thermodynamic equilibrium. The solution treated Mg9Gd alloy contains additionally a weak component with lifetime ≈ 300 ps which comes from quenched-in vacancies bound to Gd atoms [10]. From the sensitivity threshold of PL spectroscopy one can deduce that

dislocation density in both the solution treated alloys does not exceed 10^{12} m^{-2}. It is in concordance with TEM studies which revealed a low dislocation density and coarse grains [10].

The HPT deformed alloys exhibit homogeneous UFG structure with grain size around 100 nm and a high density of dislocations. The PL spectra of the HPT deformed alloys consist of two components, see Table 2. The shorter component with lifetime τ_1 comes from free positrons, while the longer component with higher intensity represents a contribution of positrons trapped at dislocations. The lifetime of $\tau_2 \approx 256$ ps agrees well with the lifetime reported previously for positrons trapped at Mg dislocations [10]. The mean dislocation density in the HPT deformed alloys shown in the last column of Table 2 was calculated from the PL results using the two-state trapping model [7] and the specific trapping rate 1×10^{-4} m^2s^{-1} [11].

Sample	τ_1 (ps)	I_1 (%)	τ_2 (ps)	I_2 (%)	ρ_D (10^{13} m^{-2})
Mg, well annealed	225.3 ± 0.4	100	-	-	< 0.1
Mg9Gd, solution tretaed	220 ± 4	91 ± 1	301 ± 2	9 ± 1	< 0.1
Mg9Gd, HPT deformed	180 ± 5	34 ± 2	256 ± 3	66 ± 2	1.1 ± 0.5
Mg4Tb2Nd, solution treated	225 ± 1	100	-	-	< 0.1
Mg4Tb2Nd, HPT deformed	180 ± 2	14.9 ± 0.4	256 ± 2	85.1 ± 0.4	3.1 ± 0.5

Table 2. A summary of PL spectroscopy results for the studied specimens.

The solution treated and HPT deformed alloys were subjected to isochronal annealing and the precipitation effects were studied. The PL spectra of the specimens are well fitted by two components at all the annealing temperatures. The shorter component with lifetime τ_1 is a contribution of free positrons, while the longer component with lifetime τ_2 comes from trapped positrons. Contrary to other techniques with equal sensitivity to all precipitates, PL spectroscopy exhibits a selective sensitivity only to precipitates capable of positron trapping. There are two kinds of such precipitates: (i) precipitates containing open-volume defects either inside the precipitate volume or at the interface with matrix (i.e. semicoherent or incoherent precipitates) or (ii) precipitates which exhibit lower (negative) affinity for positrons than the matrix (i.e. the positron energy in the precipitate is lower than in the matrix). Although the positron affinities for Gd, Tb and Nd have not been determined yet, there are strong indications that the case (ii) does not occur in the studied alloys: First, Mg exhibits rather low (negative) value of positron affinity [12] which reflect the low average electron density, lower than in Gd, Tb and Nd. Second, the lifetime of trapped positrons in both alloys remains ≈ 256 ps at all the annealing temperatures. This lifetime corresponds to vacancy-like defects in Mg and is remarkably longer than the bulk positron lifetimes for Gd, Tb and Nd. Temperature dependence of the intensity I_2 of positrons trapped at defects for Mg9Gd and Mg3Tb2Nd alloy is plotted in Fig. 1A and Fig. 2A, respectively. The behavior of microhardness in both isochronally annealed alloys is shown in Fig. 1B and Fig. 2B.

The quenched-in vacancies bound to Gd atoms in the solution treated Mg9Gd facilitate diffusion of Gd atoms and are subsequently incorporated in the coherent β'' particles formed above 80°C. The presence of open-volume defects in the β'' particles is testified by an increase of I_2 due to β'' formation in the temperature range (80-120)°C. At higher temperatures the β'' particles coarse and the associated vacancies are annealed out. Both these factors cause a decrease of I_2. The fine β'' particles represent relatively effective obstacles for movement of dislocations and cause a noticeable hardening (≈ 10%). At 200°C the β'' phase transforms into fine plates of the semicoherent β' phase precipitating on the $\{2\bar{1}\bar{1}0\}$ planes in all three possible orientation modes. It

has a slight hardening effect. Positrons are trapped in misfit defects at the semicoherent interfaces. Above 260°C two of the orientation modes dissolute whereas the particles of the remaining mode grow into oval plates with diameter around 100 nm. This explains the two-peak character of I_2 and HV dependence. Finally above 350°C coarse spherical precipitates of the stable β phase are formed and above 400°C the solid solution is restored.

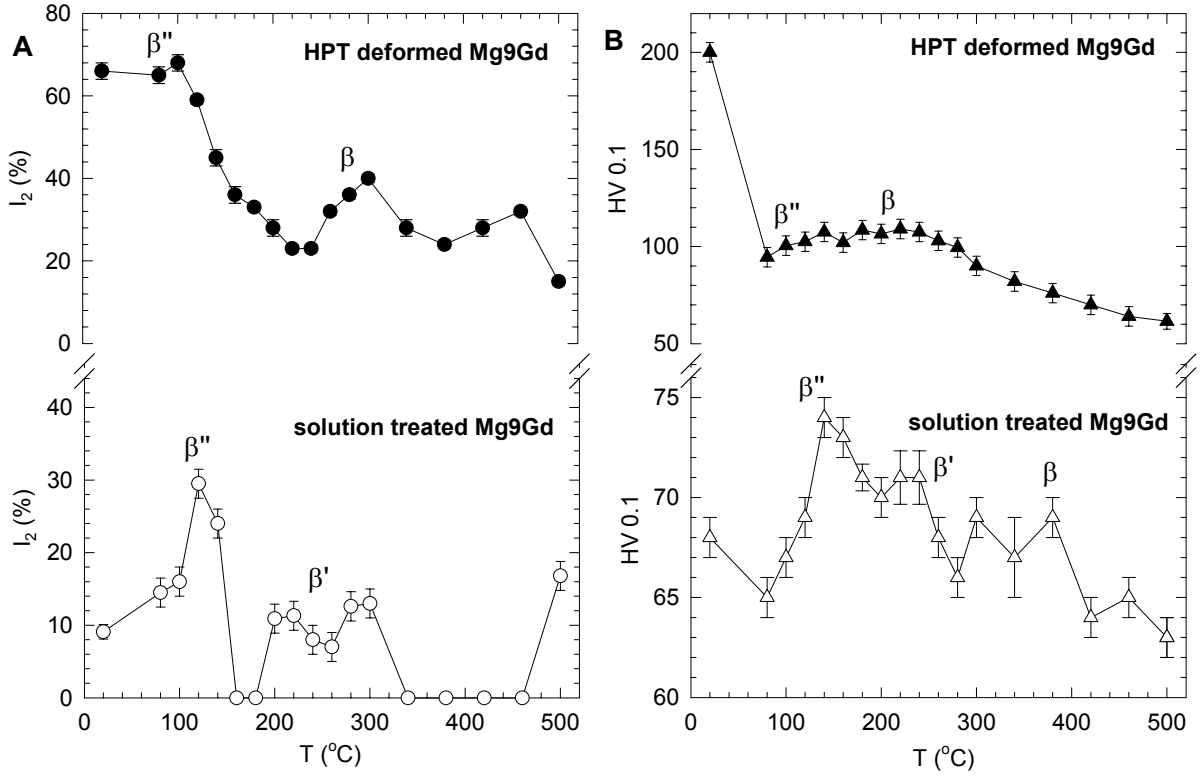

Fig. 1. Mg9Gd alloy: (A) Temperature dependence of the intensity I_2 of positrons trapped at defects (lifetime $\tau_2 \approx 256$ ps), (B) microhardness HV as a function of the annealing temperature.

Temperature development of HPT deformed Mg9Gd alloy microstructure includes not only the precipitation effects, but also recovery of defects introduced by the severe plastic deformation. Recovery of dislocations causes a drastic decrease in I_2 and HV at low temperatures. However a slight local increase in I_2 can be seen at 100°C. Similarly HV starts to increase slightly at 100°C. It is an indication of formation of the β'' phase. Thus, in the temperature range (100–220)°C two competitive processes take place in the HPT deformed Mg9Gd specimen: (i) precipitation hardening caused by the β'' particles and (ii) softening due to recovery of dislocations. At 260°C I_2 starts to increase again and it is accompanied by an additional slight hardening. It testifies precipitation of a new phase. A maximum in I_2 is attained at 300°C. The TEM observations at this temperature revealed precipitates of the stable β phase. It was found by TEM that the whole UFG grains are transformed in once into the β phase. Thus, formation of the metastable β' phase is omitted in the UFG Mg9Gd alloy and the stable β phase is formed at significantly lower temperatures. It should be mentioned that grain growth was observed only in the sample annealed above 300°C. Hence, the UFG structure in HPT deformed Mg9Gd alloy exhibits an excellent thermal stability. Coarsening of the β phase precipitates above 300°C leads to a decrease in I_2 due to increasing distance between the precipitates which reduce the probability of positron trapping.

Contrary to Mg9Gd alloy the solution treated Mg3Tb2Nd does not contain quenched-in vacancies most probably due to lower binding energy between vacancy and Tb and Nd alloying elements. One can see in Fig. 2B that precipitation of the β'' phase in the solution treated Mg3Tb2Nd alloy starts around 80°C and causes a remarkable hardening. The β'' phase particles are fully coherent with the Mg lattice and do not contain open volume defects. It is demonstrated by the fact that the solution treated Mg3Tb2Nd sample exhibits a single component PL spectrum in the

temperature range up to 280°C, i.e. there are no active positron traps in this temperature range. The TEM investigations revealed out that fine spherical β'' phase precipitates transform into fine plates in the temperature interval (180-240)°C. One can see in Fig. 2B that it has a strong hardening effect (160 %) with the peak hardness at 220°C. Fine β'' phase plates precipitate in a triangular configuration parallel with the prismatic planes $\{11\bar{2}0\}$. Further annealing up to 280°C leads to a growth of the plate-shaped precipitates (diameter 20-30 nm) reflected by a decrease in HV. At higher temperatures the β'' phase transforms into the β_1 phase with fcc structure. Plates (200-500 nm in diameter) of the β_1 phase were observed by TEM in the alloy annealed up to 330°C. The formation of the β_1 phase is accompanied by appearance of a defect component with lifetime $\tau_2 \approx$ 256 ps in PL spectra. Intensity I_2 of this component steeply increases with temperature up to a maximum at 340°C, see Fig. 2A. Thus, vacancy-like defects are created by formation of the semicoherent β_1 phase precipitates. Positrons are most probably trapped at misfit defect at the precipitate-matrix interfaces. The stable β phase precipitates from 390°C and causes also a noticeable hardening seen in Fig. 2B. Above 450°C the β phase precipitates dissolve and the solid solution is restored.

Fig. 2. Mg3Tb2Nd alloy: (A) Temperature dependence of the intensity I_2 of positrons trapped at defects (lifetime $\tau_2 \approx 256$ ps), (B) microhardness HV as a function of the annealing temperature.

The HPT-deformed Mg3Tb2Nd shows a strong decrease in I_2 caused by recovery of dislocations in the temperature range (100-180)°C, see Fig. 2A. The precipitation of the β'' phase, which takes

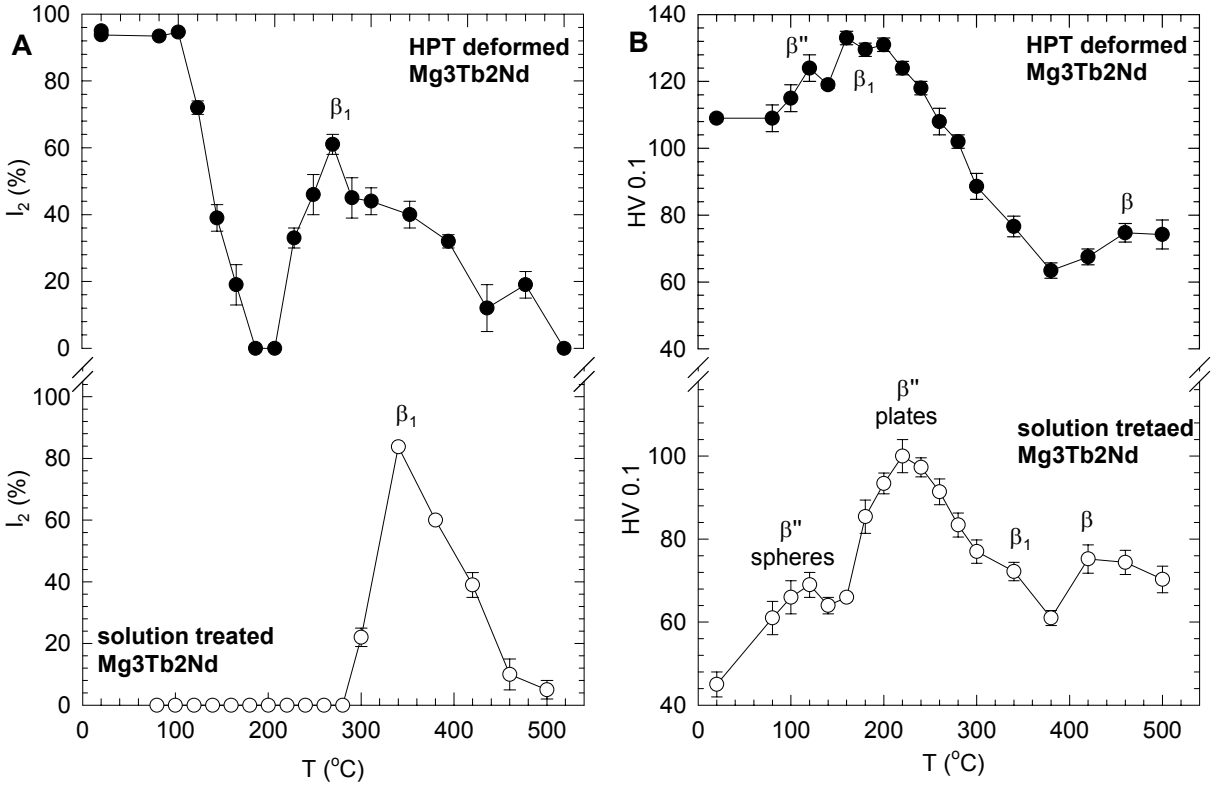

place at similar temperatures as in the coarse grained alloy, causes a remarkable hardening, see Fig. 2B. As has been already explained, PL spectroscopy is insensitive to precipitation of the coherent β'' phase. However, one can see in Fig. 2A that the intensity I_2 starts to increase in the HPT-deformed sample annealed up to 220°C and reaches its maximum at 260°C. This increase occurs due to positron trapping at defects introduced by precipitation of the semicoherent β_1 phase particles and is reflected also by an increase in HV. After annealing above 260°C, the behavior of I_2 is reversed and it gradually decreases in similar manner as in the coarse grained alloy. Thus, the precipitation of the β1 phase in the HPT deformed alloy starts at about of 80°C lower temperatures than in the solution treated sample.

Summary

The precipitation effects in coarse grained and UFG Mg9Gd and Mg3Tb2Nd alloys were compared. It was found that the precipitation sequence in the UFG alloys differs substantially from that in the corresponding coarse grained samples. The general trend is a shift of the precipitation to lower temperatures. Hence, the precipitation effects are facilitated in the UFG alloys. It has two reasons: (i) The extremely small grain size leads to a significant volume fraction of grain boundaries which provide nucleation sites for the second phase particles. (ii) Diffusivity of the alloying atoms is enhanced by a possibility to diffuse along grain boundaries and along dislocations.

Acknowledgement

This work was financially supported by the Czech Science Foundation (contract 106/05/0073) and the Ministry of Education of The Czech Republic (project No. MS 0021620834).

References

[1] B.L. Mordike: Mat. Sci. Eng. A Vol. 324 (2002), p. 103.

[2] P. Vostry, B. Smola, I. Stulikova, F. von Buch, B.L. Mordike: Phys. Stat. Sol. (a) Vol. 175 (1999), p. 491.

[3] V. Neubert, I. Stulikova, B. Smola, B.L. Mordike, M. Vlach, A. Bakkar, J. Pelcova: Mat. Sci. Eng. A Vol. 462 (2007), p. 329.

[4] J. Cizek, I. Prochazka, B. Smola, I. Stulikova, M. Vlach, R.K. Islamgaliev, O. Kulyasova, in: *Magnesium 2006*, edited by K.U. Kainer, Wiley-VCH, Weiheim (2007), p. 517.

[5] R.Z. Valiev, R.K. Islamgaliev, I.V. Alexandrov: Prog. Mat. Sci. Vol. 45 (2000), p. 103.

[6] J. Cizek, I. Prochazka, B. Smola, I. Stulikova, V. Ocenasek: J. Alloys Comp. Vol. 430 (2007), p. 92.

[7] P. Hautojärvi, C. Corbel, in: *Proceedings of the International School of Physics "Enrico Fermi", Course CXXV*, edited by A. Dupasquier, A.P. Mills, IOS Press, Varena (1995), p. 491.

[8] I. Stulikova, B. Smola, N. Zaludova, M. Vlach, J. Pelcova: Kovove Materialy Vol. 43 (2005), p. 272.

[9] F. Becvar, J. Cizek, L. Lestak, I. Novotny, I. Prochazka, F. Sebesta: Nucl. Instr. Meth. A Vol. 443 (2000), p. 557.

[10] J. Cizek, I. Prochazka, B. Smola, I. Stulikova: Phys. Stat. Sol. (a) Vol. 203 (2006), p. 466.

[11] M. Abdelrahman, P. Badawi: Jpn. J. Appl. Phys. Vol. 35 (1996), p. 4728.

[12] M.J. Puska, P. Lanki, R.M. Nieminen: J. Phys. Condens. Matter Vol. 1 (1989), p. 6081.